Adsorption of Sulfur Hexafluoride and Propane at Temperatures near Ambient on Pillared Clays

Teresa J. Bandosz, Jacek Jagiełło,† and James A. Schwarz*

Department of Chemical Engineering and Materials Science, Syracuse University, Syracuse, New York 13244-1190

The adsorption isotherms for SF_6 and C_3H_8 are reported at three temperatures near ambient on pillared clays with different gallery sizes imposed by heat treatment. X-ray diffraction experiments show a decrease in pore size (interlayer spacing) with increasing calcination temperature. Heat treatment also causes the decrease in surface areas and micropore volumes obtained from N_2 adsorption isotherms. The relationship between the two effects is discussed. An objective, mathematically rigorous, method to calculate isosteric enthalpies of adsorption is proposed. This method allows for a critical assessment in the error of the derived enthalpies based on estimates of the error in the laboratory measurement. Isotherms with complex shapes can be successfully analyzed over the entire range of the experimental variable. Using this approach, a decrease in initial enthalpies of adsorption with heat treatment is observed.

Introduction

Pillared clays, due to their catalytic applications as well as an ability to separate small molecules, have recently stimulated great interest (Pinnavaia, 1983; Occelli and Tindwa, 1983; Plee et al., 1985; Yang and Baksh, 1991; Molinar and Vasant, 1995). Their pore sizes can be modified by introducing different polycations/pillars which support silicate layers and open the interlayer gallery for molecules to penetrate. The application of these materials is limited by their basic sorption and structural characteristics. The structure of pillared clays has been studied by such physical and chemical methods as X-ray diffraction, FTIR, NMR, IGC, and potentiometric titration (Pinnavaia, 1983; Occelli and Tindwa, 1983; Plee et al., 1985; Bergaoui et al., 1995; Chevalier et al., 1994; Bandosz et al., 1992; Bandosz et al., 1994b; Bandosz et al., 1995). Nevertheless, the scientific reports describing the structural characteristics of pillared clays based on sorption experiments are limited.

Recently Baksh and Yang (1992), Gil and Montes (1994), and Gil et al. (1995) have discussed properties of pillared montmorillonites in terms of their micropore size distribution. Their results were based mainly on sorption of nitrogen.

The results reported in this paper are the part of an extended study of chemical and structural properties of pillared clays. Here we chose gas molecules that interact in a nonspecific way with a surface and can penetrate the interlayer space of materials due to their molecular diameters of about 5 Å (Hirschfelder et al., 1964). The gases chosen show significant adsorption and reach almost saturation of the pillared clays under our experimental conditions.

The objective of this paper is to report adsorption data obtained on relatively well-defined systems from the structural point of view. These data can be used to verify theoretical models of adsorption and can lead to the calculation of pore-size distributions. The advantage of using these materials to verify adsorption models is due to the fact that pore sizes of pillared clays can be measured independently by such techniques as X-ray diffraction. On the other hand, the changes occurring during heat treatment of pillared clays are very complex. Thus another objective of this paper is to underline the complexity of the pillared clays' pore structure. The interpretation of data presented here is simple. A more sophisticated analysis that leads to the adsorption energy distribution and pore size distribution based on the sorption isotherms reported in this paper is presented elsewhere (Jagiełło et al., in press).

* To whom correspondence should be addressed.
† Permanent address: Faculty of Fuels and Energy, University of Mining and Metallurgy, 30-059 Kraków, Poland.

Experimental Section

Materials. The Wyoming bentonite (Black Hill) was mixed with solutions of Chlorhydrol to intercalate large polycations into the mineral interlayer space. Chlorhydrol is the trade name of a solution of hydroxyaluminum cations manufactured by Reheis Chemical Co. The intercalation was done according to the method described elsewhere (Fahley et al., 1989; Bandosz et al., 1994a). The product of modification was washed with distilled water until the reaction to chloride ions was negative. The sample obtained was designated as W-A.

To impose the changes in the pore structure of the intercalated sample the material was heat treated at 673 and 873 K for 10 h. The samples obtained in this way are designated as W-A(673) and W-A(873), respectively. Heat treatment caused the dehydration and dehydroxylation of pillars accompanied by the shrinking of the interlayer distance (Occelli and Tindwa, 1983; Bandosz et al., 1992; Bandosz et al., 1994a).

Methods. X-ray Diffraction Analysis. Oriented clay mounts were made by settling a suspension of bentonite onto a glass slide. All clay mounts were dried at room temperature and heat treated clay mounts were rehydrated after calcination at 673 and 873 K. X-ray diffractograms were produced with a Philips PW1729 diffractometer using filtered Cu Kα radiation.

Volumetric Sorption Experiments. Adsorption isotherms were measured by a GEMINI III 2375 surface area analyzer (Micromeritics). Before the experiment the samples were heated for 10 h at 473 K and then outgassed at this

S0021-9568(95)00303-7 CCC: $12.00

Table 1. Experimental Results on the W-A Sample (Volumes of Gas Refer to p = 101.325 kPa and T = 273.15 K)

	$v(SF_6)$/cm^3 g^{-1}			$v(C_3H_8)$/cm^3 g^{-1}		
P/kPa	264.5 K	267 K	282 K	267 K	283 K	298 K
0.133	0.14	0.13	0.06	0.67	0.25	0.15
0.267	0.36	0.27	0.12	1.29	0.53	0.30
0.547	0.65	0.57	0.28	2.25	1.01	0.63
0.800	0.95	0.85	0.43	3.00	1.44	0.90
1.07	1.23	1.10	0.57	3.59	1.80	1.17
1.33	1.51	1.36	0.72	4.17	2.16	1.41
1.61	1.77	1.60	0.86	4.69	2.52	1.62
2.00	2.14	1.94	1.06	5.37	2.94	1.94
2.67	2.73	2.48	1.40	6.43	3.65	2.45
3.33	3.23	2.95	1.70	7.37	4.25	2.91
4.00	3.71	3.40	1.99	8.23	4.81	3.31
4.68	4.16	3.81	2.26	9.05	5.33	3.70
5.33	4.57	4.20	2.52	9.83	5.80	4.06
6.00	4.98	4.58	2.77	10.59	6.26	4.40
6.67	5.37	4.94	3.02	11.37	6.70	4.73
8.00	6.10	5.62	3.47	12.88	7.54	5.31
9.33	6.81	6.26	3.90	14.42	8.33	5.88
10.67	7.49	6.87	4.32	15.99	9.09	6.43
12.00	8.16	7.48	4.72	17.43	9.82	6.94
13.33	8.81	8.11	5.09	18.77	10.56	7.42
16.00	10.10	9.26	5.81	20.62	11.99	8.34
18.67	11.41	10.40	6.50	21.66	13.41	9.24
21.33	12.76	11.57	7.16	22.35	14.79	10.09
24.00	14.15	12.71	7.80	22.87	16.10	10.94
26.68	15.55	13.89	8.42	23.29	17.30	11.76
29.34	16.98	15.07	9.03	23.65	18.28	12.57
32.01	18.31	16.25	9.65	23.96	19.09	13.38
34.68	19.44	17.47	10.24	24.24	19.71	14.16
40.01	21.07	19.45	11.45	24.74	20.62	15.67
45.36	22.11	20.83	12.64	25.17	21.28	17.00
50.69	22.84	21.76	13.85	25.54	21.80	18.10
56.01	23.42	22.47	15.02	25.88	22.21	18.95
64.02	24.11	23.26	16.70	26.33	22.74	19.92
69.35	24.50	23.70	17.68	26.60	23.05	20.40
74.69	24.84	24.08	18.54	26.86	23.33	20.81
80.03	25.15	24.42	19.27	27.11	23.58	21.16
85.37	25.43	24.72	19.89	27.34	23.81	21.47
90.69	25.69	25.00	20.42	27.55	24.03	21.75
96.03	25.93	25.25	20.88	27.76	24.24	22.01
101.26	26.07	25.39	21.13	27.88	24.36	22.15

Table 2. Experimental Results on the W-A(673) Sample (Volumes of Gas Refer to p = 101.325 kPa and T = 273.15 K)

	$v(SF_6)$/cm^3 g^{-1}			$v(C_3H_8)$/cm^3 g^{-1}		
P/kPa	266.5 K	283 K	297.5 K	266.5 K	283 K	297.5 K
0.133	0.09	0.04		0.43	0.20	0.11
0.267	0.17	0.07	0.03	0.76	0.36	0.18
0.547	0.35	0.20	0.09	1.42	0.74	0.41
0.800	0.51	0.26	0.15	1.89	1.01	0.57
1.07	0.69	0.34	0.20	2.31	1.31	0.73
1.33	0.82	0.43	0.25	2.72	1.56	0.94
1.61	0.97	0.51	0.31	3.07	1.79	1.12
2.00	1.18	0.64	0.43	3.53	2.11	1.33
2.67	1.53	0.85	0.53	4.23	2.63	1.66
3.33	1.84	1.11	0.72	4.83	3.09	1.99
4.00	2.13	1.21	0.76	5.36	3.48	2.27
4.68	2.40	1.38	0.95	5.84	3.85	2.53
5.33	2.65	1.54	0.97	6.29	4.17	2.79
6.00	2.89	1.70	1.08	6.76	4.47	3.02
6.67	3.13	1.86	1.19	7.20	4.76	3.25
8.00	3.57	2.15	1.39	8.11	5.31	3.67
9.33	3.98	2.44	1.58	9.07	5.82	4.05
10.67	4.37	2.70	1.77	10.16	6.31	4.41
12.00	4.74	2.96	1.95	11.41	6.78	4.74
13.33	5.11	3.20	2.12	12.84	7.25	5.06
16.00	5.82	3.67	2.46	15.80	8.20	5.67
18.67	6.52	4.10	2.78	17.62	9.20	6.24
21.33	7.24	4.52	3.08	18.63	10.29	6.81
24.00	7.96	4.93	3.37	19.31	11.48	7.36
26.68	8.74	5.33	3.66	19.83	12.78	7.93
29.34	9.59	5.72	3.93	20.26	14.09	8.50
32.01	10.51	6.10	4.20	20.64	15.26	9.08
34.68	11.55	6.49	4.45	20.97	16.20	9.68
40.01	13.96	7.26	4.96	21.54	17.47	10.94
45.36	16.19	8.05	5.45	22.05	18.31	12.28
50.69	17.66	8.88	5.94	22.49	18.94	13.56
56.01	18.64	9.75	6.42	22.89	19.43	14.70
64.02	19.75	11.15	7.14	23.42	20.04	15.99
69.35	20.33	12.16	7.63	23.75	20.38	16.62
74.69	20.83	13.18	8.11	24.04	20.70	17.14
80.03	21.25	14.15	8.61	24.32	20.99	17.57
85.37	21.64	15.03	9.11	24.59	21.26	17.94
90.69	21.99	15.80	9.61	24.84	21.51	18.27
96.03	22.31	16.45	10.13	25.09	21.75	18.55
101.26	22.50	16.82	10.46	25.24	21.88	18.72

temperature under a vacuum of 0.001 kPa. The accuracy of pressure measurement was 0.01 kPa.

Sulfur hexafluoride and propane adsorption isotherms were measured for each sample at three different temperatures around ambient (266−298 K), which was accomplished with a homemade thermostated system controlled by a Fisher Scientific Model 900 isotemp refrigerated circulator. The stability of temperature was better than 1 K. Nitrogen adsorption isotherms were measured at 77 K. The results obtained are collected in Tables 1−3.

Results and Discussion

The results of X-ray diffraction analysis are presented in Table 4. The intercalation with hydroxyaluminum polycations caused a significant increase in the interlayer distance of bentonite compared to the initial form of material (Pinnavaia, 1983; Bandosz et al., 1994a). It is well-known that heat treatment of pillared clays results in the decrease of the d_{001} parameter due to the dehydration and dehydroxylation of pillars (Occelli and Tindwa, 1983; Bandosz et al., 1992; Bandosz et al., 1994a). Nevertheless, the X-ray results show that bentonite intercalated with hydroxyaluminum pillars is thermally stable until 873 K (Occelli and Tindwa, 1983; Bandosz, 1991).

The d_{001} parameter of the initial intercalated sample, W-A, reaches 18.4 Å which, after subtraction of the thickness of silicate layers (9.8 Å) and assuming that it is constant (Grim, 1968), gives us the accessible spacing equal to 8.8 Å in its vertical dimension. Silicate layer thickness was calculated by adding the size of one oxygen atom to the thickness of silicate layers taken from the nuclei to nuclei distance of surface oxygen (Beutelspacher and Van Der Marel, 1968). The above calculation leads to the effective size of the gallery within the mineral structure that can be accessible for the sorbate molecule. The size of the gallery was estimated in the same way for other heat-treated samples (Table 4). Table 4 indicates that there are dramatic changes in the structure of mineral that occur after heating at 873 K. At this temperature the process of dehydroxylation of hydroxyaluminum pillars is completed (Bandosz et al., 1994a) and the well-defined Al_{13} Keggin polycation is transformed into an oxide-like form of Al_2O_3 (Occelli and Tindwa, 1983).

Changes in the geometrical structure of materials are also monitored by sorption of nitrogen. From the isotherms, the surface areas S_L and S_{BET} and micropore volumes V_{mic} were calculated (Table 4) using Langmuir, BET, and Dubinin−Radushkevich equations, respectively. It is well-known that the BET method underestimates the surface area for microporous materials. In the case of our pillared clays where pore sizes do not allow for multilayer formation we consider the Langmuir method more reliable. We have also estimated the surface areas, S, of our materials directly from the micropore volumes (Table 4). Assuming a slitlike shape of pores, the surface area may

Table 3. Experimental Results on the W-1(873) Sample (Volumes of Gas Refer to p = 101.325 kPa and T = 273.15 K)

	$v(SF_6)$/cm^3 g^{-1}			$v(C_3H_8)$/cm^3 g^{-1}		
P/kPa	268.5 K	283 K	297.5 K	266.5 K	282.5 K	298 K
0.133	0.08	0.02		0.36	0.18	0.10
0.267	0.14	0.08	0.04	0.64	0.33	0.15
0.547	0.31	0.16	0.10	1.16	0.64	0.34
0.800	0.45	0.24	0.15	1.55	0.86	0.47
1.07	0.60	0.32	0.20	1.91	1.10	0.62
1.33	0.78	0.41	0.25	2.27	1.31	0.75
1.61	0.90	0.49	0.31	2.62	1.51	0.87
2.00	1.10	0.61	0.38	3.03	1.79	1.08
2.67	1.44	0.88	0.52	3.72	2.25	1.35
3.33	1.73	1.01	0.71	4.31	2.66	1.64
4.00	2.01	1.19		4.88	3.04	1.88
4.68	2.28	1.37		5.38	3.39	2.13
5.33	2.52	1.53	1.05	5.88	3.70	2.35
6.00	2.76	1.70	1.10	6.35	4.02	2.56
6.67	2.98	1.86	1.20	6.83	4.32	2.79
8.00	3.39	2.16	1.41	7.75	4.89	3.17
9.33	3.78	2.44	1.61	8.66	5.42	3.55
10.67	4.14	2.71	1.80	9.66	5.95	3.90
12.00	4.49	2.97	1.99	10.66	6.46	4.24
13.33	4.83	3.21	2.18	11.79	6.94	4.58
16.00	5.45	3.67	2.52	14.13	7.92	5.19
18.67	6.03	4.09	2.84	15.94	8.89	5.78
21.33	6.59	4.49	3.15	17.02	9.89	6.35
24.00	7.14	4.88	3.45	17.75	10.92	6.91
26.68	7.68	5.25	3.73	18.31	11.98	7.46
29.34	8.21	5.60	4.00	18.78	13.07	8.00
32.01	8.74	5.95	4.27	19.19	14.06	8.53
34.68	9.29	6.28	4.452	19.55	14.90	9.07
40.01	10.43	6.93	5.02	20.17	16.12	10.15
45.36	11.70	7.55	5.47	20.70	16.98	11.25
50.69	12.99	8.16	5.91	21.17	17.62	12.31
56.01	14.04	8.76	6.34	21.59	18.14	13.30
64.02	15.26	9.68	6.95	22.15	18.79	14.53
69.35	15.87	10.29	7.35	22.47	19.16	15.18
74.69	16.40	10.92	7.74	22.77	19.49	15.73
80.03	16.87	11.54	8.12	23.06	19.80	16.19
85.37	17.29		8.50	23.33	20.08	16.59
90.69	17.66		8.88	23.58	20.35	16.95
96.03			9.25	23.83	20.60	17.26
101.26			9.48	23.98	20.75	17.44

Table 4. X-ray Diffraction Results and Structural Parameters Calculated from Nitrogen Adsorption Isotherms

sample	gallery size/Å	d_{001}/Å	S_L/m^2 g^{-1}	S_{BET}/m^2 g^{-1}	V_{mic}/cm^3 g^{-1}	S/m^2 g^{-1}
W	3.6	12.4	30	25		
W-A	8.8	18.4	350	248	0.126	286
W-A(673)	8.0	17.6	330	223	0.113	283
W-A(873)	6.2	16.0	309	214	0.107	345

be obtained by dividing the micropore volume by the vertical pore size (from X-ray diffraction) and multiplying by 2.

It is interesting to note that due to the first step of heat treatment a decrease in V_{mic} is proportional to the decrease in spacing (about 10%), whereas in the second thermal treatment the decrease in spacing is relatively larger than the decrease in V_{mic} (30% compared to 15%). This can be explained by the fact that heat treatment at 873 K causes shrinkage of pillars in both the vertical and horizontal dimensions due to the symmetry of the Al_{13} Keggin cation (Plee et al., 1985). In addition to this some shrinkage of montmorillonite layers may also occur. These changes, we assume, compensate the decrease in the gallery size which causes the micropore volumes to not change in the same order as d_{001} for the W-A(673) and W-A(873) samples. When we compare the decrease in pore volumes with the decrease in spacing, it is seen that to compensate the difference between them, the surface area should increase about 20% in the case of the W-A(873) sample. This effect is reflected by the increase in the S value calculated from V_{mic} and pore width (Table 4).

To check if the increase of this order of magnitude is reasonable, we estimated the total surface area of the mineral occupied by pillars in the initial intercalated sample. We assume that the pillars are geometrically represented by cubes equal in size to the interlayer spacing calculated from X-ray diffraction results (e.g., 8.8 Å in height corresponds to a surface area occupied by one pillar of about 160 Å^2). Taking the charge of the Al_{13} Keggin polycation as 7^+ (Plee et al., 1985) and the surface area per unit charge in the case of montmorillonite about 70 Å^2 (Barrer, 1978), one calculates that a pillar should neutralize the charge spread over about 500 Å^2. Dividing 160 by 500, we find that pillars occupy about 32% of the total surface area of the layers. The value obtained indicates that a 20% increase in the accessible surface area of layers appears to be a reasonable number.

One has to be aware that the approach used here is simplified and does not take into account the complexity of the mineral structure, changes in the surface chemistry due to heat treatment, probably a random distribution of pillars, and a complicated shape of the Al_{13} Keggin polycation. All these factors result in existing surface heterogeneity that can be evaluated based on sorption of small molecules such as SF_6 at temperatures close to ambient (Jagiełło et al., 1995a). The detailed analysis and discussion of these effects is given elsewhere (Jagiełło et al., in press). Here we confine our discussion to the analysis of the isosteric enthalpies of adsorption.

A convenient way to calculate isosteric enthalpy of adsorption from isotherms measured at different temperatures is by using a virial-like equation (Czepirski and Jagiełło, 1989):

$$\ln p = \ln v + (1/T)\sum_{i=1}^{m} a_i v^{i-1} + \sum_{i=1}^{n} b_i v^{i-1} \qquad (1)$$

where v, p, and T are amount adsorbed, pressure, and temperature, respectively, and a_i and b_i are empirical parameters. This equation was derived under the assumption that in the limited range of temperatures the isosteric enthalpy of adsorption, Q_{st}, is temperature invariant and that the adsorption isotherms obey Henry's law in the limit of zero pressure. Fitting eq 1 simultaneously to adsorption isotherms obtained at different temperatures gives a set of temperature independent parameters a_i which lead to direct evaluation of Q_{st}:

$$Q_{st} = -R\left(\frac{\partial \ln p}{\partial (1/T)}\right)_v = -R\sum_{i=0}^{m} a_i v^{i-1} \qquad (2)$$

where R is a universal gas constant. The virial type equation was also used by Avgul and Kiselev (1970) for calculation of Q_{st}. The difference between eq 1 and their formulation was recently discussed (Jagiełło et al. 1995b). Equation 1 was successfully applied to several adsorption systems over a broad range of pressures using relatively low values of m and n (Czepirski and Jagiełło, 1989; Bandosz et al., 1993; Jagiełło et al., 1995b). However, due to the numerical instability of higher order polynomials, this equation may be used only for certain shapes of isotherms whose accurate fit does not require polynomials of higher order.

As seen from Figures 1 and 2, the adsorption isotherms of SF_6 and C_3H_8 obtained for our pillared clays show two inflection points which makes them quite complex and

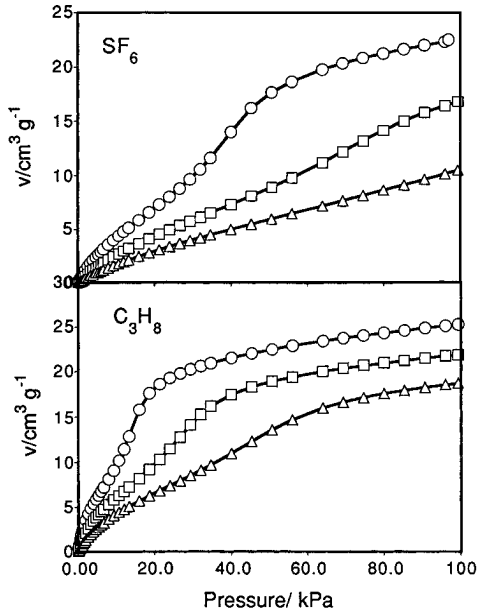

Figure 1. Adsorption isotherms of SF_6 and C_3H_8 on W-A(673):) 266.5 K; (□) 283 K; (△) 297.5 K.

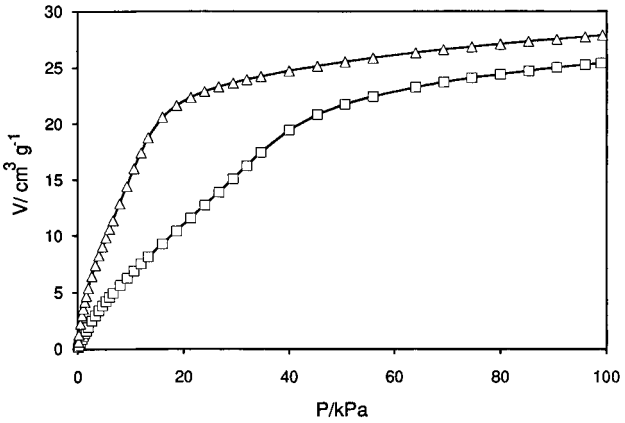

Figure 2. SF_6 (□) and C_3H_8 (△) adsorption isotherms at 267 K on the W-A sample.

difficult to fit accurately by eq 1 over the whole range of pressures. To calculate Q_{st} from such complicated isotherms, we apply the following procedure. We fit eq 1 to subsets of data points rather than to all experimental data. Each subset comprise N_s data points selected consecutively with respect to v. By considering a sequence of overlapping subsets, we scan the whole range of data. From the data of each subset we calculate one value of $Q_{st}(v_s)$ using eq 2. For the value v_s at which Q_{st} is calculated, we chose the average of the minimum and maximum values of v in the subset.

To estimate uncertainties of the calculated Q_{st} values, one needs to know the error variances, σ^2, of the p, v, and T measurements. Since σ of experimental errors are usually not known a priori, it is a common practice to estimate their values from the data. In our approach we allow for variation of σ between subsets of data and we obtain independent local estimates of σ for different subsets:

$$\sigma_p^{\,2} = (N_s - m - n)^{-1} \sum_{i=1}^{N_s} [(\ln p_i^{\exp} - \ln p_i^{eq})]^2 \qquad (3)$$

where superscripts exp and eq refer to the experimental and calculated pressures, respectively. The value σ_p

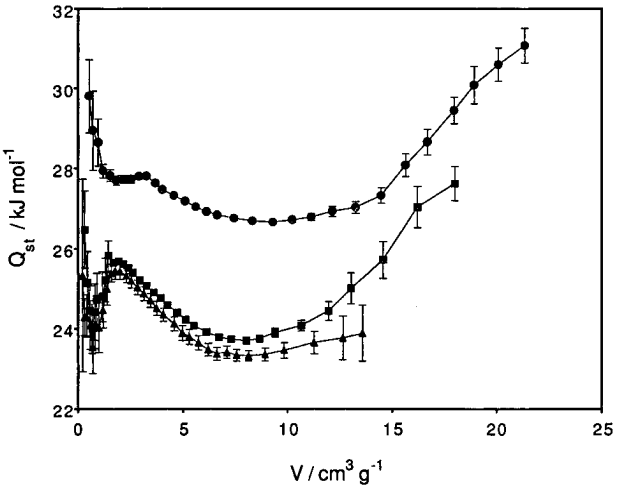

Figure 3. Enthalpies of SF_6 adsorption on pillared clays calcined at different temperatures: (●) W-A; (■) W-A(673); (▲) W-A(873).

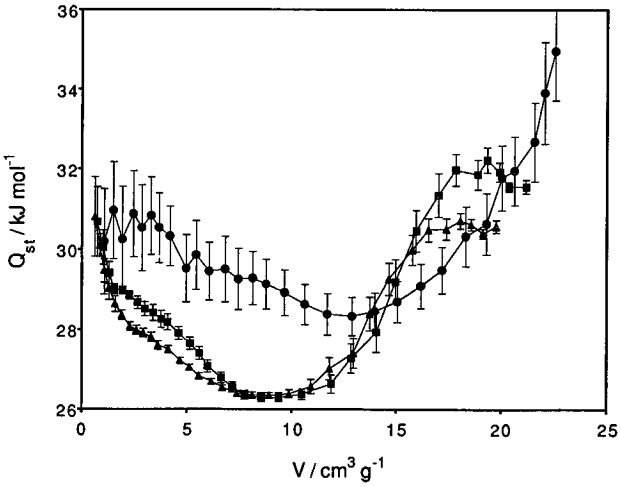

Figure 4. Enthalpies of C_3H_8 adsorption on pillared clays calcined at different temperatures: (●) W-A; (■) W-A(673); (▲) W-A(873).

characterizes the error of $\ln(p)$ which results effectively from errors of all measured variables. From σ_p, by applying the law of propagation of errors, we estimate σ_Q of the calculated $Q_{st}(v_s)$:

$$\sigma_Q^{\,2}(v_s) = \sigma_p^{\,2} \sum_{j=1}^{m} \sum_{k=1}^{m} v_s^{j-1} S_{jk} v_s^{k-1} \qquad (4)$$

where S_{jk} are the elements of the inverse matrix of the normal equations (Matrin, 1971).

The advantages of dividing experimental data into subsets, which are analyzed as samples representing local adsorption behavior, are that we can apply a simple equation to correlate the data and we can obtain local estimates of errors. The number of points, N_s, taken as a sample should be large enough to make the sample representative but not too large in order to retain a local character of the sample. In our calculations we set the size of the subset $N_s = 15$. In eq 1 we take $m = 3$ and $n = 1$. We found that these orders of polynomials are sufficient to fit the data of subsets of selected size within experimental accuracy. Increasing m and n above 3 and 1 did not change significantly the results obtained.

The calculated isosteric enthalpies of SF_6 and C_3H_8 adsorption on our samples are presented in Figures 3 and 4. Indicated error bars correspond to σ_Q values calculated from eq 4. All curves show overall a similar shape with one broad global minimum. In the case of SF_6 we observe

also local minima at low coverage; they are, however, accompanied by high uncertainties of Q_{st}. Adsorption enthalpies reflect the magnitude of the combined gas−solid and gas−gas interactions and are related to solid structure and adsorbate properties. Initial high Q_{st} values are due to adsorption on the highest energy sites; when these become saturated adsorption proceeds to sites of lower adsorption energy which correspond to a decrease in Q_{st}; subsequent increase in Q_{st} is attributed to the contribution of the lateral interaction energy between adsorbed molecules which have saturated the adsorption space. Comparing Q_{st} curves for different samples, we observe for both gases a consistent decrease in Q_{st} with the temperature of heat treatment of the sample. This indicates that structural changes in pillars and/or mineral layers occurred during heat treatment.

In conclusion, the results presented here show that the adsorption isotherms measured at different temperatures are sensitive to the changes in the structure of pillared clays induced by heat treatment. These data may be used in more advanced theoretical modeling of adsorption leading to better understanding of this process in pillared clays.

Literature Cited

Baksh, M. S. A.; Yang, R. T. Unique Adsorption Properties and Potential Energy Profiles of Microporous Pillared Clays. *AIChE J.* **1992**, *38*, 1357−1368.

Bandosz, T. Structural Parameters of Intercalated Smectite in the Light of Sorption and Other Physico-Chemical Studies. *Bull. Polish Acad. Sci.—Chem.* **1991**, *39*, 167−176.

Bandosz, T. J.; Jagiełło, J.; Andersen, B.; Schwarz, J. A. Inverse Gas Chromatography Study of Modified Smectite Surfaces. *Clays Clay Miner.* **1992**, *40*, 306−310.

Bandosz, T. J.; Jagiełło, J.; Schwarz, J. A. Effect of Surface Chemical Groups on Energetic Heterogeneity of Activated Carbons. *Langmuir* **1993**, *9*, 2518−2522.

Bandosz, T. J.; Gomez-Salazar, S.; Putyera, K.; Schwarz, J. A. Pore Structure of Carbon-Smectite Nanocomposites. *Micropor. Mater.* **1994a**, *3*, 177−184.

Bandosz, T. J.; Jagiełło, J.; Putyera, K.; Schwarz, J. A. Characterization of Acidity of Pillared Clays by Proton Affinity Distribution and DRIFT Spectroscopy. *J. Chem. Soc. Faraday Trans.* **1994b**, *90*, 3573−3578.

Bandosz, T. J.; Jagiełło, J.; Schwarz, J. A. Surface Acidity of Pillared Taeniolites in Terms of Their Proton Affinity Distributions. *J. Phys. Chem.* **1995**, *99*, 13522−13527.

Barrer, R. M. *Zeolites and Clay Minerals as Sorbents and Molecular Sieves*; Academic Press: London, 1978.

Bergaoui, L.; Lambert, J.-F.; Suquet, H.; Che, M. Cu(II) on Al_{13}-Pillared Saponites: Macroscopic Adsorption Measurements and EPR Spectra. *J. Phys. Chem.* **1995**, *99*, 2155−2166.

Beutelspacher, H.; Van Der Marel, H. W. *Atlas of Electron Microscopy of Clay Minerals and their Admixtures*; Elsevier: Amsterdam, 1968; p 42.

Chevalier, S.; Franck, R.; Suquet, H.; Lambert, J.-F.; Barthomeuf, D. Al-Pillared Saponite. Part 1. IR Studies. *J. Chem. Soc., Faraday Trans.* **1994**, *90*, 667−674.

Czepirski, L.; Jagiełło, J. Virial-Type Thermal Equation of Gas-Solid Adsorption. *J. Chem. Eng. Sci.* **1989**, *44*, 797−801.

Fahley, D. R.; Williams, K. A.; Harris, J. R.; Stapp, P. R. Preparation of Pillared Clays. U.S. Patent 4,845,066, 1989.

Gil, A.; Montes, M. Analysis of the Microporosity in Pillared Clays. *Langmuir* **1994**, *10*, 291−297.

Gil, A.; Guiu, G.; Grange, P.; Montes, M. Preparation and Characterization of Microporosity and Acidity of Silica-Alumina Pillared Clays. *J. Phys. Chem.* **1995**, *99*, 301−312.

Grim, R. E. *Clay Mineralogy*; McGraw-Hill: New York, 1968.

Hirschfelder, J. O.; Curtiss, C. F.; Bird, R. B. *Molecular Theory of Gases and Liquids*; Wiley: New York, 1964.

Jagiełło, J.; Bandosz, T. J.; Putyera, K.; Schwarz, J. A. Study of Micropore Structure of Template Derived Carbons Using Adsorption of Gases with Different Molecular Diameters. *J. Chem. Soc., Faraday Trans.* **1995a**, *91*, 2929−2933.

Jagiełło, J.; Bandosz, T. J.; Putyera, K.; Schwarz, J. A. Adsorption near Ambient Temperatures of Methane, Carbon Tetrafluoride and Sulfur Hexafluoride on Commercial Activated Carbons. *J. Chem. Eng. Data* **1995b**, *40*, 1288−1292.

Jagiełło, J.; Bandosz, T. J.; Schwarz, J. A. Heterogeneity of Pillared Clays Studied by Adsorption of SF_6 at Temperatures Near Ambient. *Langmuir*, in press.

Martin, B. R. *Statistics for Physicists*; Academic Press: London, 1961.

Molinard, A.; Vasant, E. F. Controlled Gas Adsorption Properties of Various Pillared Clays. *Adsorption* **1995**, *1*, 49−60.

Occelli, M. L.; Tindwa, P. M. Physicochemical Properties of Montmorillonite Interlayered with Cationic Oxyaluminium Pillars. *Clays Clay Miner.* **1983**, *31*, 22−28.

Pinnavaia, T. J. Intercalated Clay Catalysts. *Science* **1983**, *220*, 365−371.

Plee, D.; Borg, F.; Gatineau, L.; Fripiat, J. J. High-Resolution Solid-State ^{27}Al and ^{29}Si Nuclear Magnetic Resonance Study of Pillared Clays. *J. Am. Chem. Soc.* **1985**, *107*, 2362−2369.

Yang, R. T.; Baksh, M. S. A. Pillared Clays as a New Class of Sorbents for Gas Separation. *AIChE J.* **1991**, *37*, 679−686.

Received for review November 30, 1995. Accepted April 30, 1996.[⊗] We would like to thank one of the reviewers for his comments regarding errors in the calculated Q_{st}. We believe that the reader is given a clear quantitative understanding of Q_{st} as determined.

JE950303M

[⊗] Abstract published in *Advance ACS Abstracts,* June 15, 1996.